Int. J. Electrochem. Sci., 10 **(2015)** 8150 - 8157

International Journal of
ELECTROCHEMICAL
SCIENCE
www.electrochemsci.org

Short Communication

Contribution of Randomly Oriented Li_2WO_4 with Tetragonal Symmetry to Li^+ Ion Transfer Resistance Reduction in Lithium-Ion Batteries

Tetsutaro Hayashi[1,2,*], *Eiji Toda*[1], *Ryuichi Kuzuo*[1], *Yasutaka Matsuda*[2], *Naoaki Kuwata*[2],
Junichi Kawamura[2]

[1]Sumitomo Metal Mining Co., Ltd, Battery Research Laboratories, 17-3, Isoura-cho, Nihama, Ehime, 792-008, Japan
[2]Tohoku University Institute of Multidisciplinary Research for Advanced Materials, Tohoku University, Katahira 2-1-1, Aoba-ku, Sendai, 980-8577, Japan
[*]E-mail: Tetsutaro_Hayashi@ni.smm.co.jp

Received: 9 June 2015 / *Accepted:* 25 June 2015 / *Published:* 26 August 2015

In this study, we used pulsed laser deposition to fabricate a thin-film electrode of $LiCoO_2$ (LCO) modified with lithium tungsten oxide (LWO). Then, to investigate the mechanisms underlying the low interfacial resistance of the modified electrode, we determined the diffusion coefficients of the Li^+ ions in the bare and LWO-modified LCO and the three-dimensional structure of the LWO. Using electrochemical impedance spectroscopy, we determined that the LWO modification of the LCO enhanced the diffusion coefficient of the Li^+ ions. XRD analysis showed that the LWO adopted a randomly oriented Li_2WO_4 structure with tetragonal symmetry displaying multiple Li^+ ion diffusion paths, which contributed to enhancing the diffusion of Li^+ ions between the positive electrode surface and liquid electrolyte, resulting in reduction of resistance to interfacial Li^+ ion transfer.

Keywords: Positive electrode, Lithium-ion battery, Surface modification, Low resistance, lithium tungsten oxide

1. INTRODUCTION

Lithium-ion batteries (LIBs) are widely used as power sources in electric and hybrid electric vehicles because they provide high power with low resistance. However, defects in LIB performance reportedly stem from hindered Li^+ ion diffusion at the interface between the positive electrode and electrolyte [1–3]. Lithium tungsten oxides (LWOs), such as Li_2WO_4 and $Li_2W_2O_7$, have been reported to be the conductors of lithium ions [4,5], and the LWOs deposited on positive electrode materials have been reported to reduce the interfacial resistance of LIBs [6,7]. One mechanism for reducing resistance is that LWO modification provides a protective layer that suppresses Co dissolution from the surface of LCO and deters accumulation of deposits such as phosphates at the interface by preventing the surface of the LCO thin film from reacting with the electrolyte [7]. Furthermore, with the LWO modification, another contribution to reduced resistance may be related to the lithium-ion conductor. However, the mechanism for this possibility remains unclear. To develop high-powered LIBs, complete understanding must be gained regarding the mechanisms underlying low interfacial resistance resulting from the LWO modification.

To investigate the mechanisms associated with the lowered resistance following the LWO modification, we fabricated the bare and LWO-modified LCO thin-film electrodes by pulsed laser deposition (PLD) and determined the diffusion coefficients of the Li^+ ions in the bare and LWO-modified LCO and the three-dimensional structure of the LWO.

2. EXPERIMENTAL PART

2.1. Fabrication of the bare and LWO-modified LCO

The details of the sample fabrication procedure are described in our previous study [7]. The LCO powder was calcined at 1000 °C for 24 h to produce the LCO target material. The bare LCO thin film was deposited on a $Pt/Cr/SiO_2$ substrate. The bare LCO was grown by PLD with a Nd:YAG laser on the LCO target material at 500 °C under an O_2 atmosphere of 20 Pa. The thickness of the bare LCO was 200 nm. The LWO was then deposited on the bare LCO thin film electrode by PLD using an ArF excimer laser at 500 °C under an O_2 atmosphere of 20 Pa. Subsequently, the bare and LWO-modified LCO thin films were deposited on substrates, both 8 mm × 8 mm in size.

2.2. XRD measurement

The bare and LWO-modified LCO thin films were then characterized by XRD. We analyzed the lattice constants and crystallite sizes using an XRD instrument (X'Pert PRO MPD, PANalytical) equipped with a Cu Kα source e, and conducted the XRD measurements using ω-2θ scanning geometry.

2.3. Electrochemical impedance spectroscopy measurement

The details of the electrochemical tests are also described in our previous study [7]. Coin cells were assembled with the bare and LWO-modified LCO thin film electrodes, a lithium metal, a $LiPF_6$-based electrolyte, and a polypropylene separator in an argon-filled glove box. We then charged the assembled coin cells to 4.0 V at a charging rate of 2.1 $\mu A\ cm^{-2}$ and analyzed the diffusion coefficient of the Li^+ ions of the positive electrodes by electrochemical impedance spectroscopy (EIS). The amplitude voltage was 10 mV and the frequency range was from 0.05 Hz to 100,000 Hz.

2.4. Determination of the three-dimensional structure of the LWO

The images of the three-dimensional crystal structures of the LWO were created using VESTA software [8].

3. RESULTS AND DISCUSSION

3.1. Structural characterization of the LWO-modified LCO

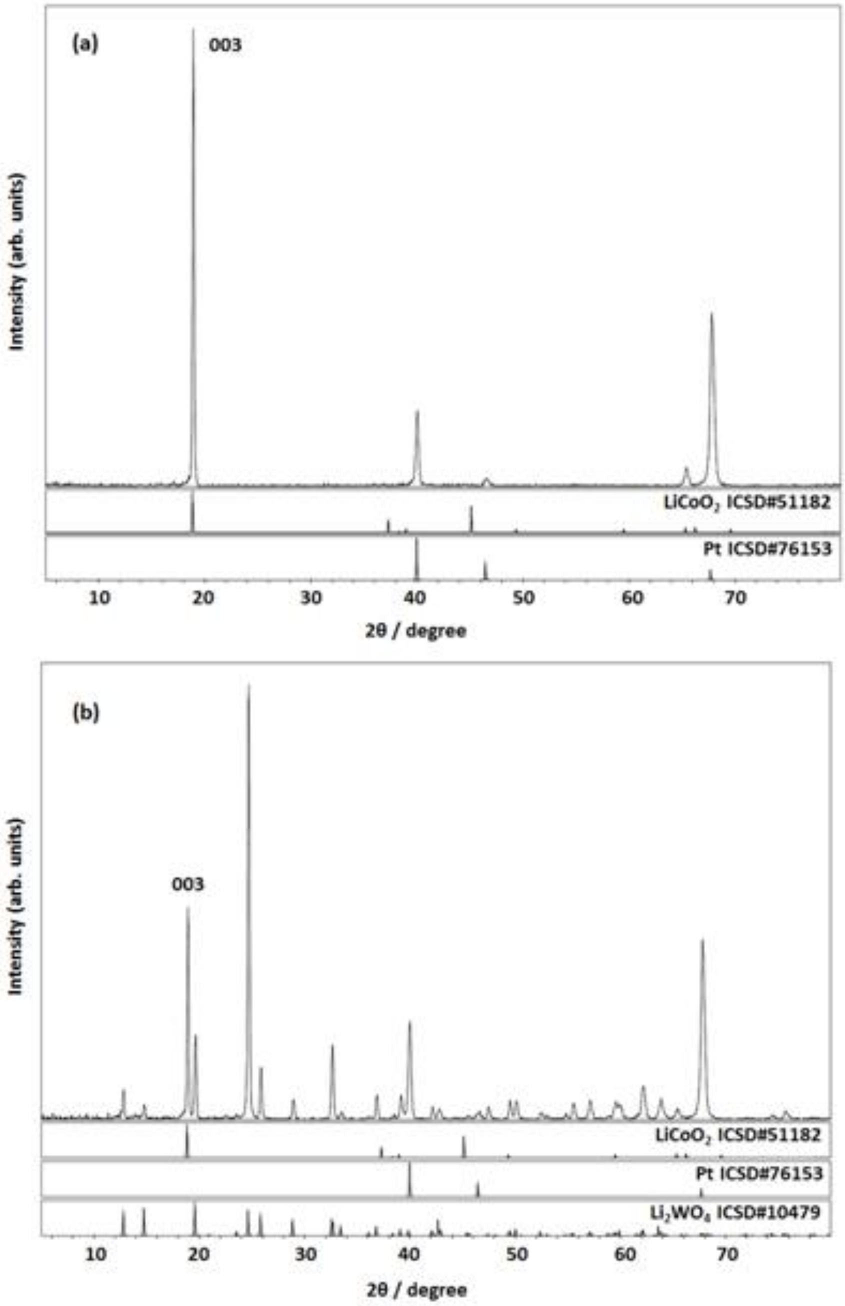

Figure 1. XRD patterns of (a) the bare LCO and (b) LWO-modified LCO.

To investigate the effect of the LWO modification on LCO structure, we determined the lattice constants and crystallite sizes of the bare and LWO-modified LCO based on the XRD data (Fig. 1). The LCO crystal structure of the bare and LWO-modified LCO were *c* axis-oriented $LiCoO_2$ with hexagonal symmetry (ICSD # 51182), as reported previously [7]. The LWO crystal structure of LWO-modified LCO was characterized by randomly oriented Li_2WO_4 with tetragonal symmetry (ICSD # 10479).

Table 1. Lattice constants *c* and crystallite sizes *t* corresponding to the (003) reflection diffraction peaks for the LCO crystal structures of the bare and LWO-modified LCO.

	C (Å)	*t* (Å)
Bare LCO	14.078(3)	566(2)
LWO-modified LCO	14.081(3)	565(2)

Table 1 shows the lattice constants *c* and crystallite sizes *t* corresponding to a (003) reflection diffraction peak for the LCO crystal structure based on the XRD data (Fig. 1). The lattice constant *c* was calculated by Bragg's law [9]:

$$n\lambda = 2d\sin\theta, \qquad (1)$$

where *n* is an integer, *λ* is the wavelength of incident X-rays, *d* is the lattice constant, which indicates the spacing between planes in the atomic lattice, and *θ* is the Bragg's angle that corresponds to the (003) reflection of the LCO structure. The (003) crystallite size was calculated by Scherrer's equation [9]:

$$t = k\lambda/(B\cos\theta), \qquad (2)$$

where *t* is the crystallite size, which indicates the mean size of the crystalline domains, *k* is a shape factor, and *B* is the full width at half maximum corresponding to the (003) reflection diffraction peak of the LCO. The bare and LWO-modified LCO present almost the same values for the lattice constants *c* and crystallite sizes *t*, indicating that no tungsten had been doped in the LCO lattice and that the LCO crystal structure was little influenced by the LWO modification. These results suggest that the low resistance of the LWO-modified LCO may be attributed to the LWO layer rather than the LCO layer.

3.2. Electrochemical effects of the LWO modification

To investigate the role of the LWO layer, we used EIS to compare the diffusion coefficients of the lithium ions in the bare and LWO-modified LCO.

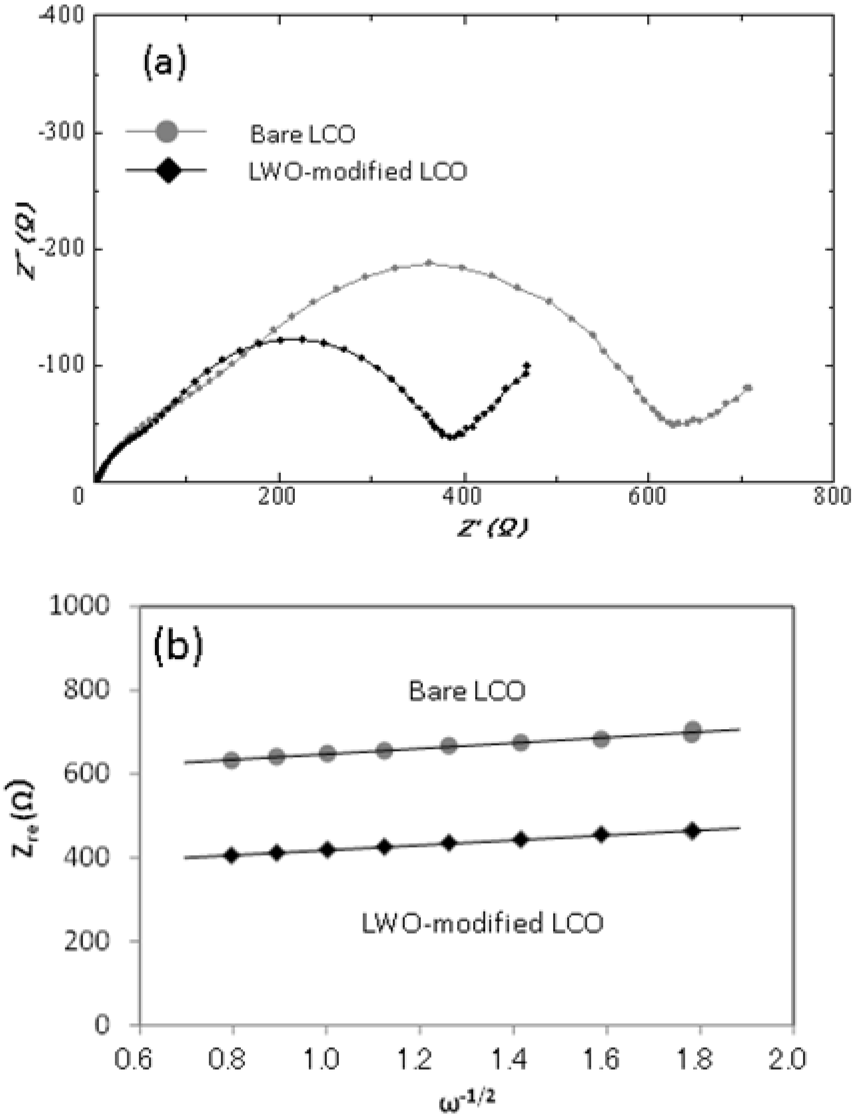

Figure 2. (a) Alternate current impedance spectra of the bare and LWO-modified LCO. (b) Relationship between Zre and $\omega^{-1/2}$ in the low frequency region.

Figure 2(a) shows the impedance spectra of the bare and LWO-modified LCO. Both spectra show two semicircles at high and intermediate frequencies and a straight line corresponding to the Warburg element at low frequencies. The diffusion coefficients of the Li^+ ions can be calculated from the plots in the low frequency region according to the following equation [10]:

$$D = R^2T^2/(2A^2n_0^4F^4C^2\sigma^2), \qquad (3)$$

where D is the diffusion coefficient, R is the gas constant, T is the absolute temperature, and A is the area of the interface between the positive electrode and electrolyte. In Eq. (3), n_0 is the number of electrons per oxide molecule, F is the Faraday's constant, C is the concentration of Li^+ ions, and σ is the Warburg factor, which is related to Z_{re}:

$$Z_{re} = R_s + R_1 + R_{ct} + \sigma\omega^{-1/2}, \qquad (4)$$

where R_s, R_1, and R_{ct} are the ohmic, surface film, and charge transfer resistances, respectively, in our proposed equivalent circuit [7], and ω is the frequency. The relationship between Z_{re} and the reciprocal square root of ω in the low frequency region is shown in Fig. 2(b). The diffusion coefficients of the Li^+ ions in the bare and LWO-modified LCO were calculated from Eq. (3) to be 2.2×10^{-13} and 3.0×10^{-13} $cm^2\ s^{-1}$, respectively. These results suggest that the LWO modification slightly enhanced the diffusion coefficient of the Li^+ ions at the positive electrode. Because the LCO crystal structure was hardly influenced by the LWO modification (Table 1), this difference in the diffusion coefficients may be attributed to the LWO rather than to any internal difference in the LCO.

3.3. Three-dimensional structure of the LWO

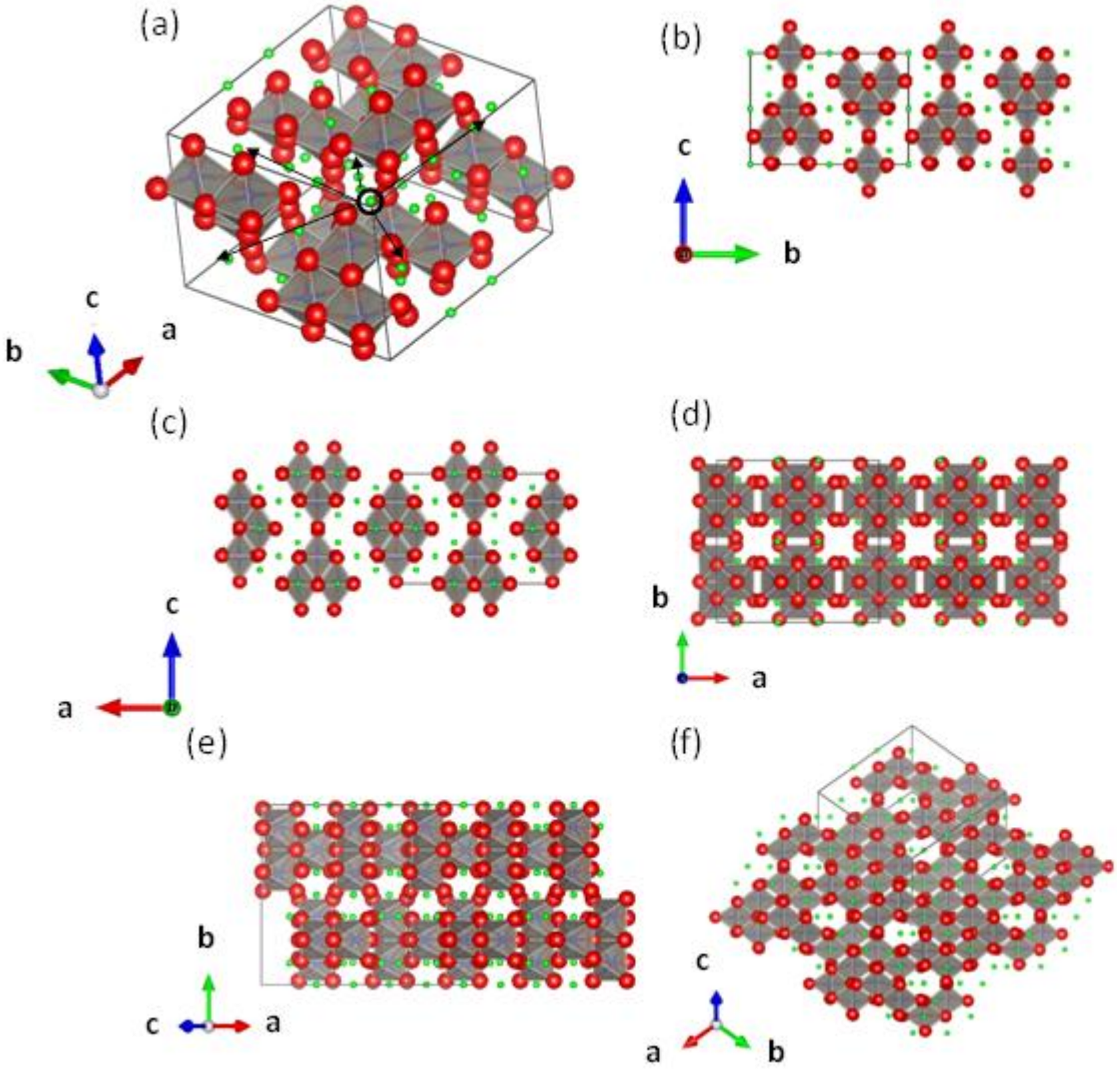

Figure 3. Three-dimensional models of tetragonal Li_2WO_4 (ICSD # 10479) drawn using VESTA software [8]. The red, blue, and green balls represent oxygen, tungsten, and lithium ions, respectively. (a) Li^+ ions (black circle) can move in different directions (arrows) through channels formed by WO_6 octahedra. The crystal structures are observed along the (b) [100] orientation, (c) [010], (d) [001], (e) [101], and (f) [111] orientations.

To clarify the ability of lithium-ion diffusion in the LWO, we investigated the LWO’s three-dimensional structure.

Figure 3 shows the three-dimensional representations of the tetragonal Li_2WO_4 symmetry (ICSD # 10479) [Fig. 1(b)], which were drawn using VESTA software [8]. Figure 3(a) shows that the LWO unit cell is consists of WO_6 octahedra that provide channels for the Li^+ ions (shown by the circle) to move along at various orientations (shown by arrows). Li^+ ions can diffuse along [100], [010], [001], [101], and [111] orientations, because the structures provide Li^+ ion diffusion paths [Figs. 3(b)–3(f)]. Therefore, the randomly oriented LWO modification may contain numerous Li^+ ion diffusion paths that facilitate ion intercalation and de-intercalation in various directions at the interface between the LWO and liquid electrolyte. In contrast, the interface between *c* axis-oriented bare LCO [Fig. 1(a)] and electrolyte may provide significantly fewer diffusion paths.

Yamada et al [11]. have investigated the effect of the LCO orientation on Li^+ ion transfer and revealed that random orientations result in lower charge transfer resistance (R_{ct}) than that associated with the (003) orientation, and that the activation energy of interfacial Li^+ ion transfer does not depend on the orientation of the LCO. Our previous results [7] indicate that the activation energy is independent of the charge transfer resistance. This result agrees with those reported by Yamada et al [11].

Moreover, in our previous study [7], the LWO-modification-induced increase in the frequency factor contributed to the lowering of the charge transfer resistance, which is also consistent with the reports by Yamada et al. [11]. This suggests that random orientations lead to significantly higher frequency factors than those associated with the (003) orientation. In general, the randomly oriented α-NaFeO-type layered LCO structure exhibits a larger number of Li^+ ion diffusion paths than does the (003) orientation. Ogumi [2] has proposed that the frequency factor depends on the number of reaction sites for Li^+ ion transfer at the positive electrode interface. Based on the assumption that the diffusion paths correlate with the number of reaction sites for interfacial Li^+ ion transfer, increasing the number of these paths may enhance the frequency factor in randomly oriented LCO, which can also be applied to the randomly oriented Li_2WO_4 with its numerous diffusion paths (Fig. 3). Hence, an increase in the number of Li^+ ion diffusion paths may contribute to the higher frequency factor for the LWO-modified LCO compared to that for the bare LCO [7]. This mechanism will contribute to lowered charge transfer resistance, in addition to suppression of Co dissolution and prevention of accumulation of deposits, such as phosphates, by preventing the surface of the LCO thin film from reacting with the electrolyte, observed in our previous study [7]. Therefore, LWO modification increased the frequency of interfacial Li^+ ion transfer, thereby facilitating ion diffusion between the positive electrode surface and liquid electrolyte and reducing interfacial Li^+ ion transfer resistance.

4. CONCLUSIONS

To investigate the mechanisms of the lowered resistance associated with the LWO modification, we fabricated an LWO-modified LCO, and determined the diffusion coefficients of the Li^+ ions in the electrode and the three-dimensional structure of the LWO. The EIS measurement results demonstrated that the LWO modification of the LCO enhanced the diffusion coefficient of the Li^+ ions. XRD analysis results showed that the LWO modification created randomly oriented Li_2WO_4 with tetragonal symmetry. The crystal structure of this Li_2WO_4 exhibited many Li^+ ion diffusion paths that enhanced the frequency factor in LWO-modified LCO and the diffusion of Li^+ ion between the positive electrode surface and liquid electrolyte, resulting in reduction of resistance to interfacial Li^+ ion transfer.

References

1. K. Amine, C. H. Chen, J. Liu, M. Hammond, A. Jansen, D. Dees, I. Bloom, D. Vissers, G. Henriksen, *J. Power Sources* 97 (2001) 684.
2. Z. Ogumi, *Electrochemistry* 78 (2010) 319.
3. T. Hayashi, J. Okada, E. Toda, R. Kuzuo, N. Oshimura, N. Kuwata, J. Kawamura, *J. Electrochem. Soc.* 161 (2014) A1007.
4. K. Nassau, A. M. Glass, M. Grasso, D. H. Olson, *J. Electrochem. Soc.*127 (1980) 2743.
5. A. H. Yahaya, Z. A. Ibrahim, A. K. Arof, *J. Alloys Compd*. 241 (1996) 148.
6. R. Kokado, K. Mori, M. Tkagi, T. Hayashi, U.S. Patent (2015) No.0021518.
7. T. Hayashi, J. Okada, E. Toda, R. Kuzuo, Y. Matsuda, N. Kuwata, J. Kawamura, *J. Power Sources* 285 (2015) 559.
8. K. Momma, F. Izumi, *J. Appl. Cryst*. 44 (2011) 1272.
9. B. D. Cullity, Elements of X-ray Diffraction, Addison-Wesley, Reading, Massachusetts (1978).
10. J. Zhao, L. Wang, X. He, C. Wan, C. Jiang, *Int. J. Electrochem. Sci*. 5 (2010) 478.
11. I. Yamada, Y. Iriyama, T. Abe, Z. Ogumi, *J. Power Sources* 172 (2007) 933.